MICROSCALE HYDRAULIC HELICAL ACTUATOR FOR CARDIOVASCULAR PROCEDURES

By

Sophia Saya Sevic

A capstone project submitted for Graduation with University Honors

May 9, 2024

University Honors
University of California, Riverside

APPROVED

Dr. Jun Sheng
Department of Mechanical Engineering

Dr. Richard Cardullo, Howard H Hays Jr. Chair
University Honors

ABSTRACT

Pulmonary emboli are one of the most common causes of deaths annually. When patients undergo anticoagulant therapy, they may either experience long-term health effects or even experience another PE. Therefore, surgical interventions have been introduced to remove PEs. There are several commercially available surgical tools that remove PEs by using catheters to deliver thrombolytic agents to lyse the clot. However, some patients may have contraindications to the delivered drugs, so patients opt to have their PEs removed mechanically. However, the tip of the catheter that physically breaks apart PEs can only move in low degrees of freedom, which could result in some fragments getting left behind in the vessel since the catheter cannot press the fragments against the surface area of the vessel. Additionally, tips made with metal meshes pose harm to the vessel tissue. Our research presents the design and fabrication of a hydraulic helical soft actuator aimed at enhancing surgical catheters to remove pulmonary emboli (PE). Our research progressed from a macroscale to microscale actuator to validate the design and fabrication process that produces the coiling mechanism. At the macroscale level, the actuator's optimal shape, chamber size, materials, and power supply-coiling relationship were determined, showing that the actuator starts performing a clear coiling motion after 10 mL of air is supplied. Validating and testing the macroscale actuator allows us to apply the fabrication procedure to a microscale actuator in a similar manner. However, an additional step to create the microscale actuator is needed, which is creating a mold made of an alternative material. Currently, we are in the process of determining how this mold should be created. Getting past this step will allow us to move forward to apply the same macroscale fabrication procedure to the microscale actuator. This research offers a comprehensive and methodical approach to developing a soft robotic actuator that is compatible with the human body and capable of effectively removing PEs.

ACKNOWLEDGMENTS

I would like to sincerely thank my faculty mentor, Dr. Jun Sheng, for welcoming me into his lab and allowing me to gain research experience in a field I am passionate about. I would not have learned the fundamentals of research and what it takes to be an engineer without his persistent support and guidance. I would also like to thank my Ph.D. student mentor, Harry Lee, for mentoring me throughout this research project by providing unique perspectives on how to enhance our prototypes and teaching me some of the hands-on skills needed for this research, such as handling silicone, using CAD software, and using the 3D printer. Next, I would like to thank my research partner, Steven Vu, for helping with the microscale actuator fabrication and trying new methods to enhance the fabrication process. Lastly, I would also like to thank the Division of Undergraduate Education for awarding me the $1,000 Mini-Grant to fund the materials essential for progressing in my research.

TABLE OF CONTENTS

INTRODUCTION

Every year, 1 in 1000 people experience a pulmonary embolism (PE), a severe cardiovascular disorder where a blood clot forms in the pulmonary arteries (PAs)[1]. PEs originate from the formation of a deep vein thrombosis (DVT), which typically forms in the legs[2]. Once a DVT enters the bloodstream, it passes through the right side of the heart and gets stuck in the PAs, causing a PE to occur[2]. 70% of people who experience a PE die within the first hour[3]. When patients experience a PE, they typically undergo anticoagulant therapy for three months[4]. However, patients either suffer from long-term after-effects, such as venous valve damage, or 9%-26% of patients experience another PE within the three months of anticoagulant therapy[5, 6].

Rather than relying on anticoagulants itself, methods of removing PEs through surgical equipment have been introduced, such as catheter-directed interventions (CDI), surgical embolectomies, and systemic thrombolysis[7]. CDI can be broken down into two categories: catheter-directed thrombolysis (CDT) and catheter-directed embolectomy (CDE)[7]. CDT uses catheters to arrive at the site of the PE and delivers a thrombolytic agent to lyse the clot[8, 9]. Whereas, CDE uses catheters to arrive at the site of the PE and mechanically lyse the clot[7]. Equipment used for CDTs, such as the FlowTriever® (Inari Medical, Irvine, CA, USA) and AngioJet™ (Boston Scientific, Marlborough, MA, USA), possess a mortality rate of 1.9% and 4.3%, respectively[10, 11]. However, some patients who experience PEs may have contraindications to thrombolysis. Therefore, CDEs become an option for patients with severe PE. For example, balloon catheters, such as the Fogarty® arterial balloon embolectomy catheter (Edwards Lifesciences, Irvine, CA, USA), are used to treat PE by being placed at the site of the PE and repeatedly inflate and deflate to break apart the clot into coarse pieces to recanalize the

vessel[12, 13]. While balloon catheters are a minimally invasive surgical tool and are easy to insert into the PAs, there are risks of size mismatches between the balloon catheter tip size and the size of the patients PA, and residual thrombus may remain in the PA as a result[13, 14]. Another more commonly used tool for CDEs is pigtail catheters. Pigtails catheters, such as SuperTorque™ (Cordis Corporation, Miami Lakes, FL, USA), are used by manually rotating the distal end of the catheter shaft around the axis of the inserted guidewire back and forth to fragment the PE[13]. Pigtail catheters are also a minimally invasive surgical tool and easy to insert into the PA, but they are only capable of moving in two dimensions, which also results in residual thrombus remaining in the PA since the catheter cannot move in a third dimension to press the fragments against the walls of the PA. Additionally, catheter shafts consist of metal meshes to enhance torque transmission of the shaft[15]. Using metal may pose risk to patients' vessels because the material is rigid, which does not easily adapt to confined spaces and could tear the vessel wall if the metal breaks. Since the mortality rate after pulmonary embolectomies is 27.2%, the surgical equipment used for CDEs continue to be researched and improved[16]. Specifically, researchers target the tip of the catheters that perform PE fragmentation to improve mechanical removal of PEs.

Surgical equipment has evolved to become less invasive, and one method to create minimally invasive surgical (MIS) tools is applying robotics. In recent years, surgeons have utilized robotic surgical equipment since they provide greater precision and more consistent quality than humans can perform[17]. While robotic surgical equipment has paved the way for new equipment and procedures to be developed, most robotic tools feature hard and rigid bodies, which lack flexibility and adaptability. However, researchers have found recently that robots made of soft, flexible materials are safe to interact with humans, possess adaptability, cause less

stress on vessel walls, have simpler fabrication methods, are easy to manipulate, and are low cost in manufacturing[18, 19].

This research aims to develop a micro-scale soft robot to fragment PE and facilitate PE removal. We will develop a soft robotic manipulator that can be navigated through vena cava into pulmonary veins using the guidewire technique, inserted into the center of a PE and transformed into a helical shape to fragment the PE (Figure 1). The helical motion of the robot will be caused by a string being wrapped in the center of the soft robot body as water is supplied to the robot due to the interaction of soft materials. The goal of this research is to test the feasibility of the design ideas and evaluate the motion capability of prototypes for PE fragmentation.

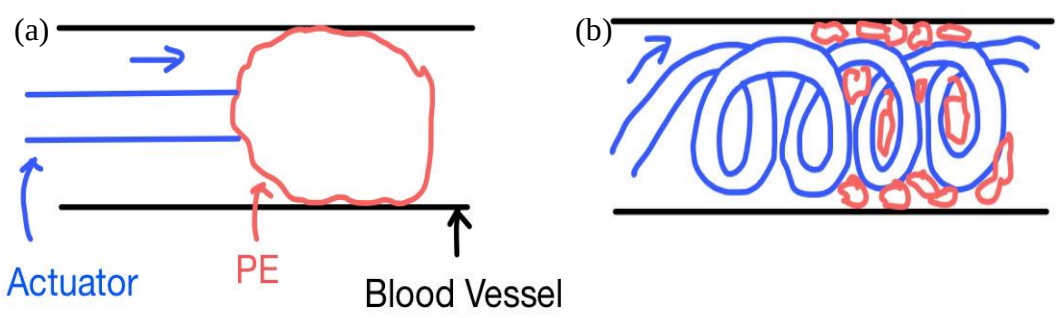

Figure 1. (a) Diagram of the application of our actuator, where the actuator is approaching the PE in a blood vessel. (b) Diagram of the actuator coiling and breaking apart the PE.

DESIGN AND FABRICATION OF THE MACROSCALE ACTUATOR

We first created a macroscale actuator to determine which fabrication procedure is the most optimal and repeatable to produce the greatest amount of coiling. After determining and testing the most optimal design, we applied the methodology to create a scaled-down version of the actuator so the actuator can fit in a pulmonary vein.

General Principle Of Helical Motion

Soft robotic actuators are capable of performing a variety of motions, such as bending, coiling, twisting, etc. These deformations can occur due the soft material properties, asymmetric structures, pressure distribution, and sequential activation. Soft materials, such as silicone, rubber, and fabric, are typically used due to their ability to change shape and how load and power is distributed, so they can adapt to changing environmental conditions[20, 21]. To make the actuator move non-linearly, chambers can be created within the actuator[22]. For example, chambers that are shaped diagonally may be created throughout the actuator tube. Depending on the shape of the chambers, such as the diagonal shape, the actuator can become asymmetrical in appearance. Therefore, when pneumatic or hydraulic pressure is supplied, the pressure distribution is different depending on whether pressure is passing through a chamber or in between two chambers. Pressure is supplied at one open end of the actuator and travels until it reaches the closed end of the tube. As a result, the pressure is supplied in a wave-like pattern along the actuator, making the actuator create the non-linear pattern as chambers and the space in between two chambers are activated one at a time. Creating diagonally shaped chambers at 45° angles produces the maximum angular displacement of coiling[22]. 3D-printing an actuator with chambers is one of the many methods to create a helical actuator (Figure 2)[18]. Another method to create helical motion is to route a string around the body of the actuator. Routing a string is a

fiber-reinforcement strategy that causes elastomeric bodies to simultaneously bend and twist, which creates the helical shape[23].

While creating diagonally shaped chambers is essential to making the actuator coil, another essential component to achieve the 3D shape is including a strain limiting layer. The strain limiting layer can be made of inextensible fabric or plastic to act as an elongation restriction on one side of the actuator, which causes the bending of the actuator when pressurized[24]. Since our actuator needs to be fabricated at the microscale level, creating a mold with a small cavity is more optimal for our purpose. Therefore, rather than 3D-printing a microscale actuator, our actuator is made using a mold that can aid in casting and curing soft material. One side of the actuator body has a strain-limiting layer attached to it, and a string is routed around the actuator and strain-limiting layer. The strain-limiting layer and fiber reinforcements work together to limit elongation and promote bending and twisting, ultimately creating the coiling mechanism, because of how the pressure interacts with the soft material with the fiber reinforcements and strain-limiting layer present.

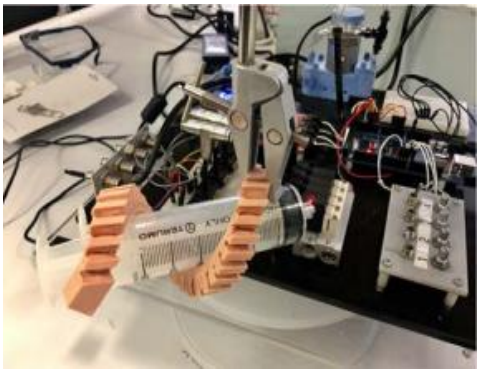

Figure 2. Example of a 3D-printed soft robot with angled chambers coiling as pressure is applied. This robot's application is for gripping objects[18].

Design Details/Procedures

Our actuator is primarily fabricated with Dragon Skin 10 Medium silicone (Smooth-On Inc., Macungie, PA, USA) due to its strong yet flexible material properties. The shape of the actuator will consist of a mostly circular shape on one side and the other side being flat (Figure 3a). The flat side of the actuator is the surface for the strain-limiting layer to be placed to restrict elongation (Figure 3b). A piece of plastic bag (Amazon Basics, Seattle, WA, USA) serves as the strain-limiting layer due to its inextensible properties and encourages more bending and coiling of the actuator when supplied with water[24]. Finally, we tightly routed the polyester string, due to its high tensile strength, around the actuator and strain-limiting layer to create 45-degree-angled chambers (Figure 3c). The result after the fabrication is shown in Figure 3d.

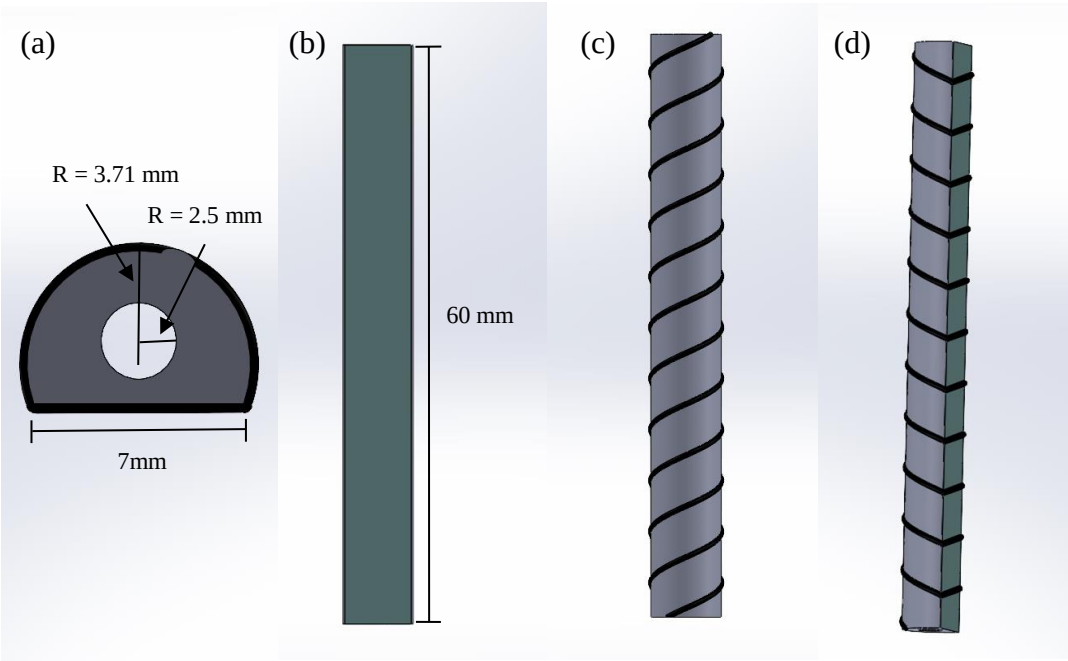

Figure 3. (a) Bottom view of the actuator showing a shape slightly more semicircular. The main actuator body is made of silicone, represented in grey. (b) Placing a piece of a plastic sandwich bag on the flat side of the actuator, represented in green. (c) Routing the string at 45-degree angles, represented in black. (d) Side-view of the final result, showing each component of the actuator.

Fabrication Methods

The actuator tube itself was made by designing and 3D-printing a mold consisting of multiple components and filling the mold with silicone because we could design and revise the shape of the mold to create an actuator that contributes to producing a great amount of coiling. The components of the mold were designed in SolidWorks, shown in Figure 4. To print the mold components, we used the Stratasys Objet30 3D-printer and VeroWhitePlus resin (Stratasys, Eden Prairie, MN). The silicone is prepared and poured into the mostly circular opening in the mold component in Figure 4a. The rod (Figure 4b) is placed on the rectangular bed in Figure 4a to allow the rod to float in the center of the cavity of Figure 4a to create the pressure supply chamber of the actuator. The rod does not extend to the end of the component in Figure 4a because we need one side of the actuator closed. The assembled rod and mostly circular wall are placed in a box (Figure 4c) to ensure the silicone does not leak from the sides between the wall and the cap. The assembly is placed in a vacuum chamber to remove air bubbles. Once the air bubbles are removed, the silicone is left to cure. The final assembly of the mold is shown in Figure 4d, and a cross-sectional view is shown in Figure 4e.

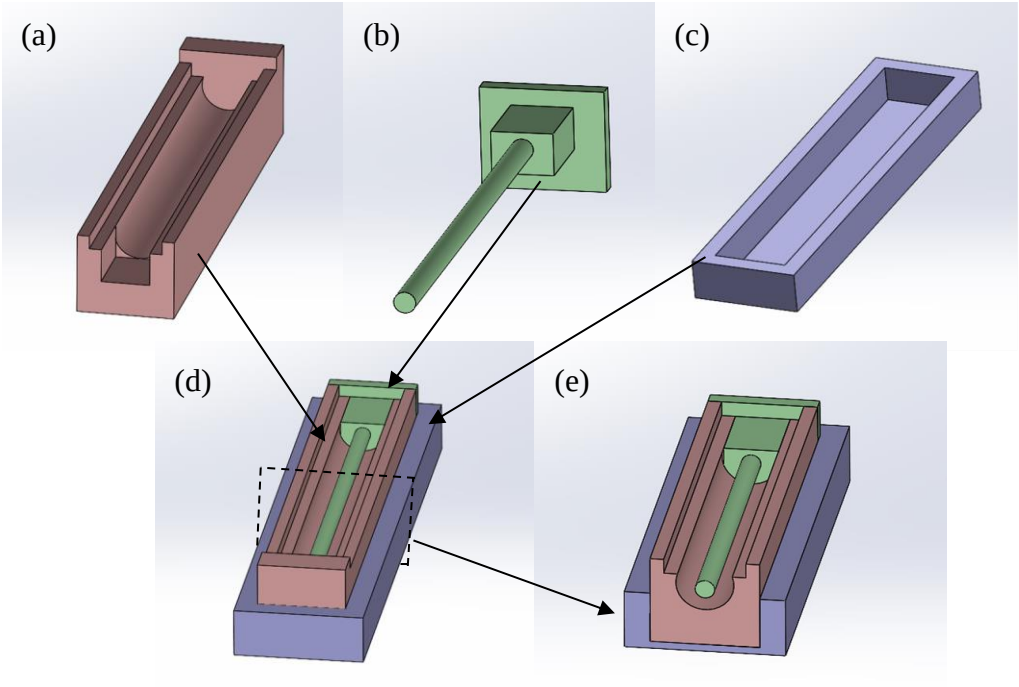

Figure 4. The components of the mold to cast silicone. (a) A wall with a circular opening to create the shape of the actuator chamber. (b) A rod attached to a extruded rectangle that matches the geometry of the rectangular nest in (a). (c) Box to tightly hold (a) and (b) together. (d) Assembly of all the mold components. (e) Cross-sectional view of the assembled mold, where the cavity is filled with silicone.

After the silicone is cured, the mold is taken apart by taking Figure 4a and b out from the box and carefully peeling the rod off from the mostly circular wall to obtain the actuator chamber wrapped around the rod (Figure 5a). Leaving the silicone on the rod, we used super glue to paste the piece of a plastic sandwich bag on the flat side of the actuator (Figure 5b). After the super glue dried, we routed the polyester string at 45° angles to create the chambers (Figure 5c). After the super glue on the string dried, we slowly removed the complete actuator off the rod.

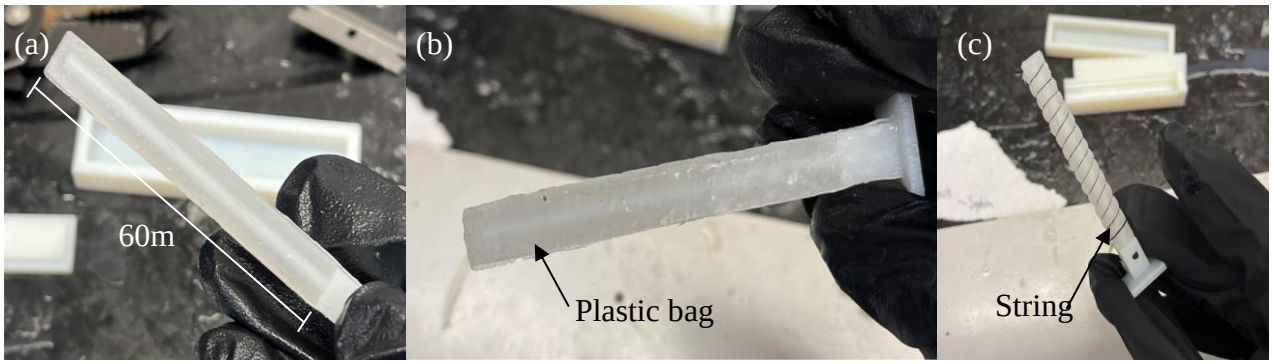

Figure 5. Steps after silicone has cured. (a) Cured silicone on the rod after taking apart the mold. (b) Applying the plastic bag on the flat side of the actuator. (c) Routing the string at 45° angles around the circular part of the actuator.

Discussion Of Outcome

The results are shown in Figure 6. The slight twisting in Figure 6a and b is due to the tension of the string routed around the actuator. Note that the top and bottom have excess string hanging from the edges, which is there in case the super glued string detaches from the silicone and needs to be reattached. Figure 6c shows the more than semi-circular shape of the actuator and the circular-shaped power supply chamber. In Figure 6d, the actuator is supplied with a small amount of air to test and show the coiling mechanism of the actuator more easily. The actuator coils clockwise, where the flat side of the actuator faces away from the camera when no power is supplied. As power is supplied, the actuator coils so the flat side ends up facing towards the camera, and the end of the actuator rotates more as more air is supplied (Figure 6e).

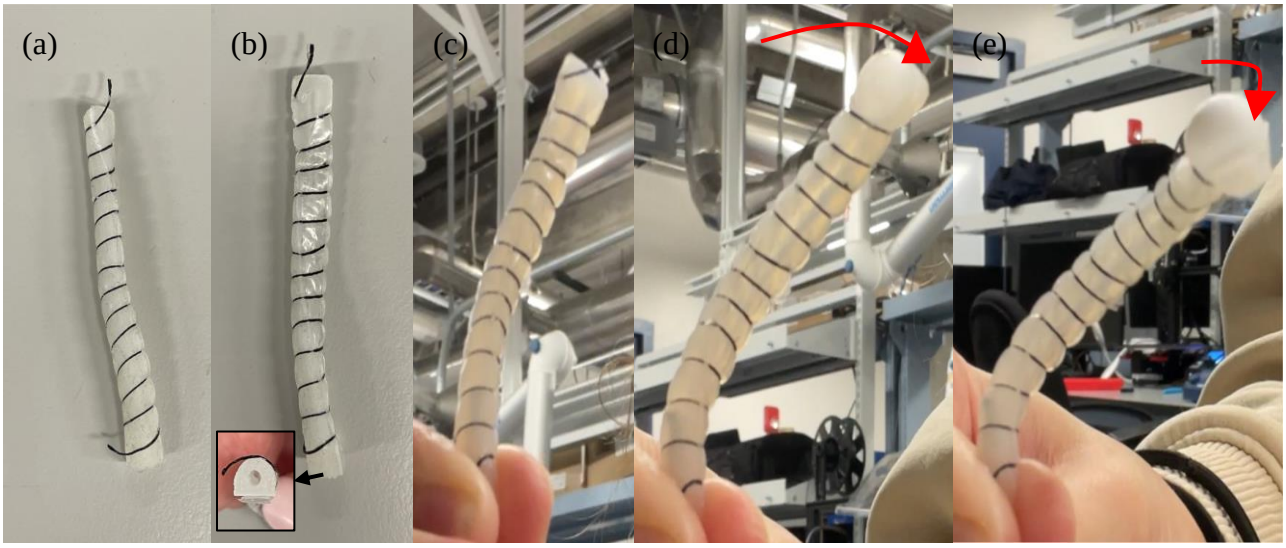

Figure 6. Results of the actuator after fabrication. (a) View showing the circular side of the actuator. (b) View of the actuator showing the flat side of the actuator and the cross-sectional view to show the mostly circular shape of the actuator and the circular power supply chamber. (c) Actuator standing vertically without power being supplied via syringe. (d) Actuator starting to coil clockwise with air as the power supply via syringe. The red arrow represents the direction the actuator is coiling with respect to the initial state. (e) More coiling clockwise as the end of the actuator points more towards the camera as more power is supplied. The red arrow represents the tip of the actuator rotates towards the camera with respect to the previous position in (d).

While determining the optimal fabrication procedure, we ran into various challenges using the silicone, such as silicone delamination, degassing, and tearing. Initially, we wanted to add a second layer of silicone around the chamber with the plastic bag and string to keep the plastic bag and string in place. However, the second layer would not stick to the original silicone layer, in other words, delaminate (Figure 7a). A possible source for delamination is due to dust accumulating on the original layer. With dust accumulating on the surface of the original layer, there was less surface area for the second layer of silicone to fully adhere to the original layer. Therefore, we decided to not add a second layer of silicone around the original layer, and the actuator was still capable of performing helical motion. While casting the silicone, we placed mold filled with silicone in a degassing chamber to remove air bubbles from the silicone. Air bubbles cause the material to become thinner, which increases the likelihood of the silicone to

tear. However, while the chamber degassed the silicone, the silicone would start to cure before all the air bubbles were removed. This would result in the actuator body having thin areas of silicone, which would tear while taking the mold apart (Figure 7b). To solve this problem, we would pop the remaining bubbles at the surface after the chamber degassed most of the bubbles but before the silicone's pot life ended so that the silicone can become more level after the surface bubbles popped.

We also encountered problems with designing and orienting the mold. In one of the prototypes, the rod that floats in the center of the circular mold cavity was not centered (Figure 7c). After fixing the measurements on SolidWorks for how far above the cavity the was supposed to float, we were able to make the power chamber centered in the actuator. Additionally, one factor we needed to consider is that the removal of the actuator should be smooth and not tear the actuator. In previous prototypes, we made the rod a semicircular shape, similar to the main shape of the actuator. The prototype in Figure 7a and b shows that the rod is semicircular. However, the likelihood of the silicone tearing was higher because of the sharp edges on the semicircle rod. Therefore, we changed the rod's shape to circular, which allowed the silicone to come off the rod more smoothly and allowed more power to be supplied in the actuator. Another issue we faced was the leakage of silicone. Because of how viscous the material is, when pouring the silicone on to the circular cavity, some of the silicone would overflow onto and over the edges of the mold. Therefore, when adding the rest of the mold components to the component already filled with silicone, the mold would not completely close due to the excess silicone on the edges. We introduced fitting the mold components into a tight box so to help press the excess silicone out from the cracks between the components and to prevent further leakage. These challenges we faced allowed us to approach the fabrication

process from different angles, ultimately leading us to find a procedure that takes minimal time and material to fabricate the actuator.

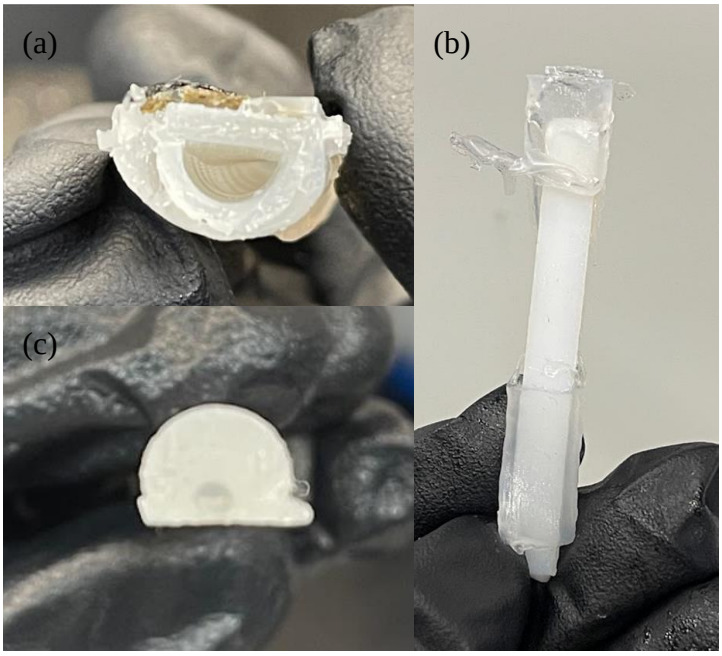

Figure 7. (a) Delamination between two layers of silicone. (b) Silicone tearing due to the layer being extremely thin. (c) Rod curing off center within the actuator.

EXPERIMENTS AND DEMONSTRATIONS

Experimental Setup

The amount of coiling the actuator can perform is due to how much power is supplied. To determine the relationship between power supply and amount of coiling, we set up an experiment to measure how much the actuator coils in three-dimensional space as power is discretely supplied into the actuator. For this experiment, we used air as the power supply instead of water since water was weighing down the actuator and water posed a potential hazard to the EM tracker setup. The power supply was set up by mounting a syringe onto a platform that moves bidirectionally via step motor (Figure 8). The bidirectional movement, forward and backward, allows the syringe to supply air to or remove air from the actuator, respectively. The step motor was connected to an Arduino circuit and a DC power supply (Shenzhen Hanma Precision Technology, Shenzhen, China). The amount of air that the syringe pumped was controlled through the Arduino code. One end of a tube was connected to the actuator while the other end was attached to a Luer lock that is screwed into the Luer lock of the syringe. We designed and 3D-printed fixtures to hold the pneumatic power system and connecting tube in place and to ensure that the system does not move as the step motor rotates.

To measure the coiling displacement of the actuator, we attached the actuator to the Aurora® electromagnetic (EM) tracking system by taping a sensor, that measures displacement in three-dimensional space, to the tip of the actuator (NDI - Northern Digital Inc., Waterloo, Ontario, Canada) (Figure 8). A field generator was placed under the actuator with the sensor so the generator can measure where the sensor is in space. The field generator and sensor were connected to the system control unit (SCU) and sensor interface unit (SIU). We ran three trials of supplying air to the actuator in 1 mL increments (Figure 9).

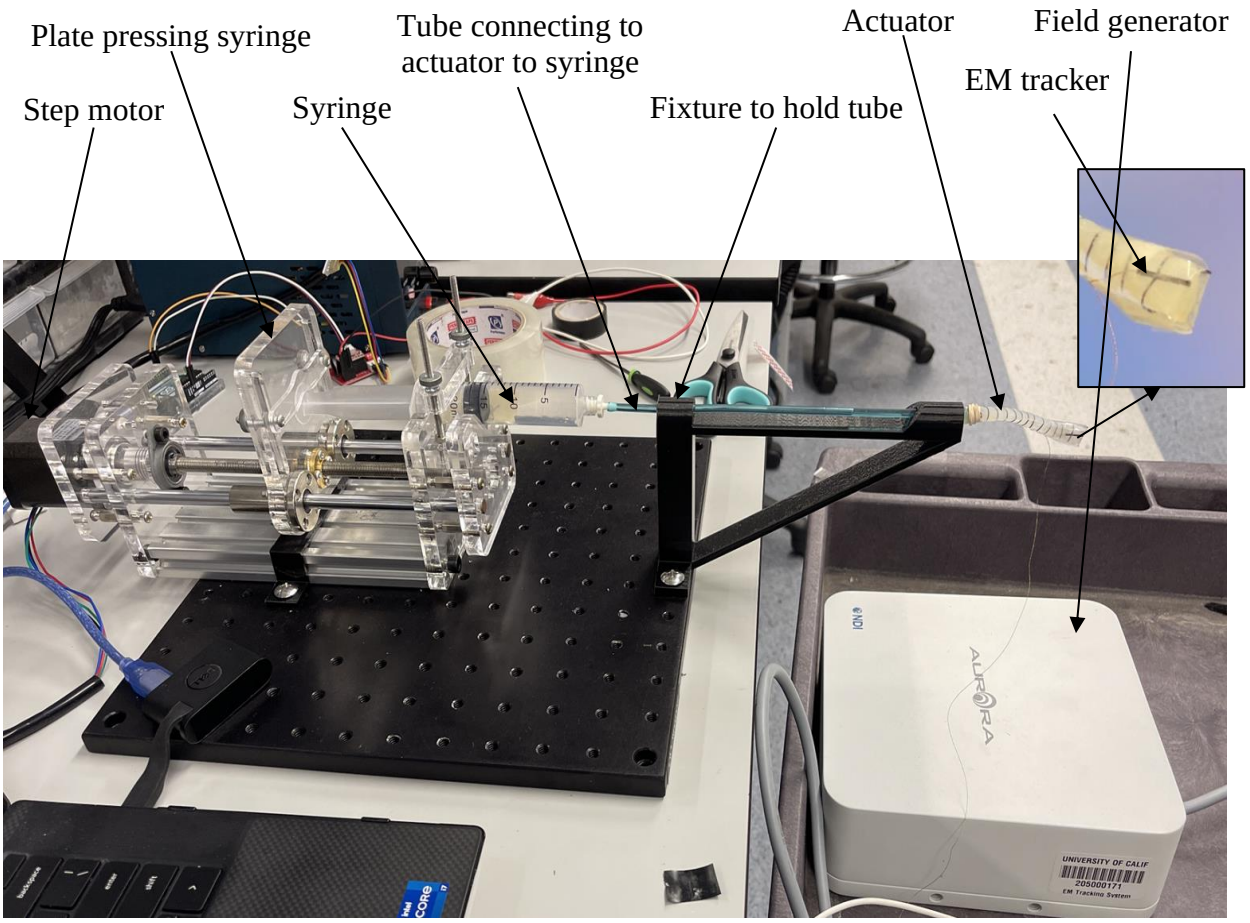

Figure 8. Testing setup consisting of a hydraulic power supply mounted onto a fixture plate (left) and an EM tracker attached to the tip of the actuator to measure the displacement and angle of the actuator in space (right).

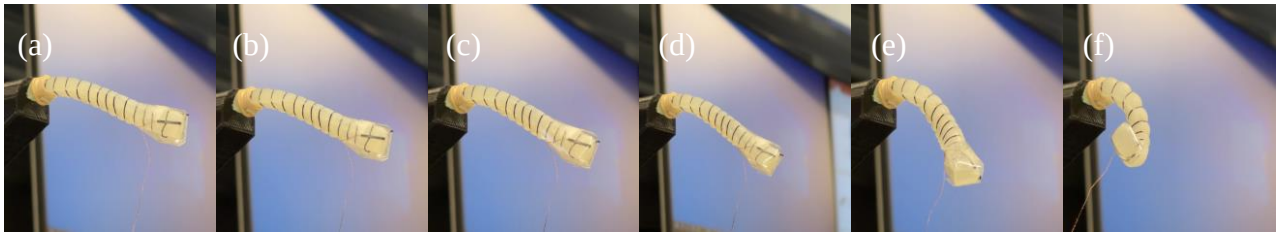

Figure 9. Actuator coiling as (a) 0 mL, (b) 5 mL, (c) 10 mL, (d) 11 mL, (e) 14 mL, and (f) 15 mL of air is supplied to the actuator.

Results and Discussion

The displacement and Euler angular rotation of the actuator coiling and uncoiling are shown in Figures 10 and 11.

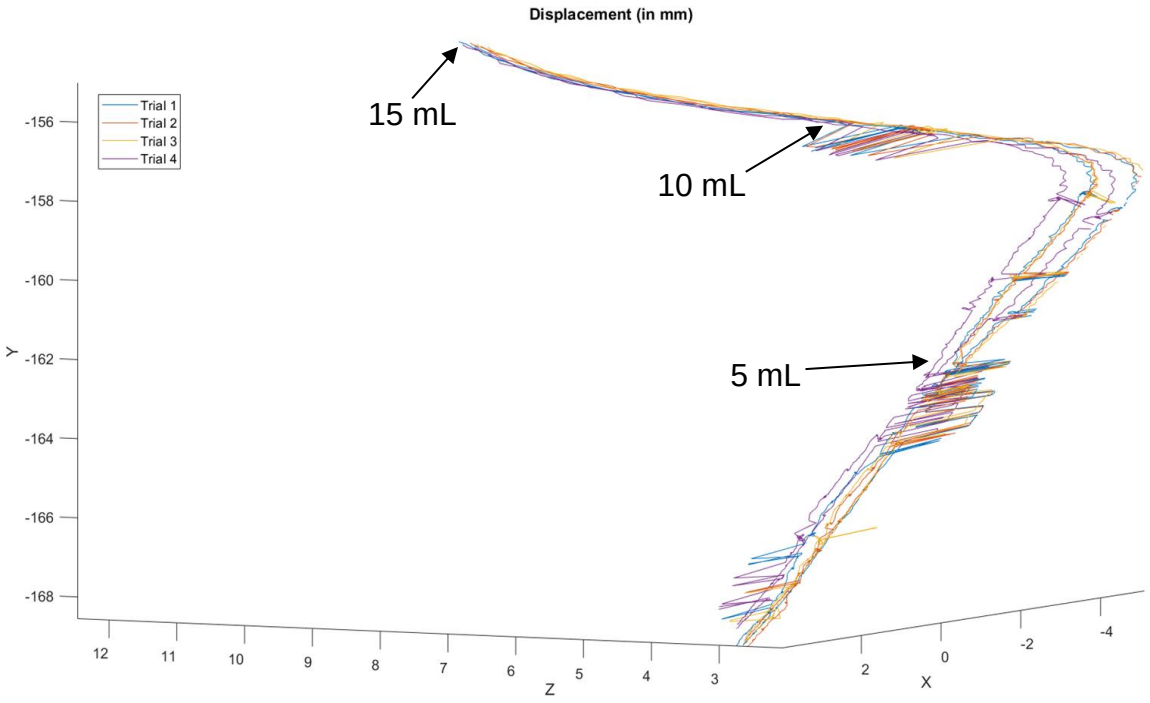

Figure 10. Displacement graph showing the trajectory of the actuator in space. The base of actuator is aligned along the x-axis, moves down along the y-axis, and curves to the left along the z-axis, where moving towards the field generator is the positive direction.

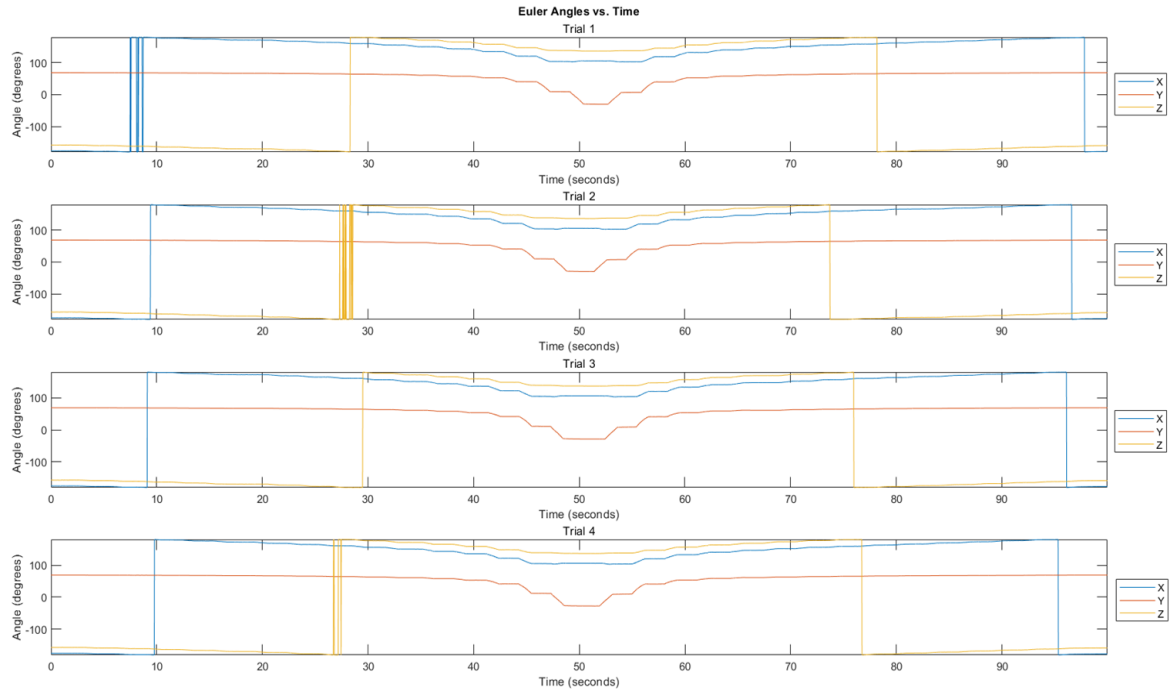

Figure 11. Euler angle graphs showing rotations about the x, y, and z axes, respectively, for all four trials. The angles indicate how much the object has rotated around each axis since its initial orientation.

The figures show that the field generator mirrored the orientation of the actuator. Figure 10 shows that the base of the actuator is aligned along the x-axis. With respect to the base, forward and backward are along the x-axis, up and down are along the y-axis, and left and right are along the z-axis. As air was supplied, the tip of the actuator moved forward and slightly downward towards the field generator, and then coiled to the left and further downward. Then, as air was retracted from the actuator, the tip of the actuator followed the same pattern to uncoil. There are some gaps in the curves due to the sensor and field generator losing connection at certain frames.

Figure 11 displays the orientation of the actuator in space. The three angles, X, Y, and Z are plotted against time to show how the orientation of the actuator changes over time. The X angle represents the rotation around the x-axis, also known as the roll. As time increases, more pressure is added, and the angle decreases until 15 mL is added, reaching the halfway point of the time interval. The angle decreasing means that the actuator is rolling counterclockwise, which is what the actuator displayed in real-time with respect to the base and field generator. The Y angle represents how much the actuator is pitching. The graph displays that the Y angle decreases as time increases until 15 mL of air is added, meaning that the actuator pitches downward. The Z angle represents how much the actuator is yawing. The yaw occurs to the left since the graph also displays the Z angle decreasing as 15 ml of air is added and time increases. After 15 mL of air is added, and the syringe starts to retract the air, the X, Y, and Z angles show an increase for the roll, pitch and yaw, representing the actuator moving in the opposite direction. Thus, the graph correctly displays the actuator coiling and uncoiling as power is supplied and removed as time increases.

The first 5 mL of air that was supplied showed that the actuator did not displace forward or coiled to the side by a lot of millimeters but rather shook side to side as air was supplied. This may be due to how the air flowed through larger then smaller chambers as it started to fill the volume of inside the actuator, and the alternating between flowing through large and small chambers caused the tip of the actuator to vibrate side-to-side based on which chamber the air was flowing through. Once the majority of the actuator was pressurized, adding more air allowed the actuator to coil due to the asymmetrical, diagonally-shaped chambers deforming. With respect to the x-axis, the actuator coiled downward towards the field generator and counterclockwise. The most coiling occurred after 10 mL of air was supplied, but some vibration still occurred approaching 10 mL. Therefore, as air starts to fill up the inside of the actuator chamber, the first 10 mL of air fill up the majority of the chamber, and the following increments of air cause the actuator to deform, resulting in a rapid increase of motion as more air is supplied. Figure 11 further displays the rapid increase by showing the visible steps after the additional 5 mL of air was added after the first 10 mL of air was added. Adding 15 mL of air shows the beginning of the coiling mechanism. The actuator may have potential to coil more with more air being supplied, but to test the full coiling capacity of the actuator, multiple samples would need to be created to test the actuators until failure.

DESIGN AND FABRICATION OF THE MICROSCALE ACTUATOR

After finalizing the fabrication process for the macroscale actuator and testing its capability to coil when water is supplied, we moved onto scaling the size of the actuator down, by applying the same procedure of casting and curing silicone in a mold, attaching the plastic bag sheet to serve as the strain limiting layer, and routing the string around the actuator to create the angled chambers.

Design Details/Procedures

The microscale actuator follows the same shape and design as the macroscale actuator but scaled down to fit within a pulmonary vein (Figure 12). The actuator is also fabricated with silicone, a piece of a plastic sandwich bag, and polyester string.

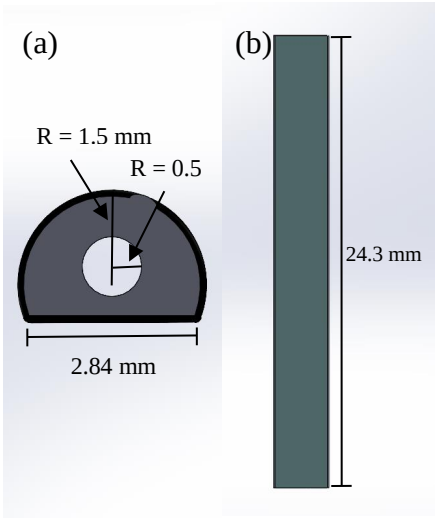

Figure 12. (a) Bottom view of the actuator with the same shape but different dimensions from scaling down. (b) New height of the actuator.

Fabrication Methods

Fabricating the microscale actuator faces many challenges due to its size and how thin the silicone layer needs to be. As mentioned in section 2.4, while determining the optimal fabrication

macroscale procedure, we noticed that peeling off thin layers of silicone from the 3D printed mold causes the silicone to tear more easily due to the high friction between the silicone and the mold. Therefore, for the microscale actuator, the actuator's mold is made of Smooth-Cast 327, a two-part polyurethane (PU) plastic (Smooth-On Inc., Macungie, PA, USA)[25]. To create the PU plastic mold, we designed and 3D-printed another multi-piece mold to hold two glass slides and a rod in between the slides (Figure 13). Using glass allows the PU plastic mold to be debonded from the mold more easily[25]. There are two main components of the mold. The first component is the base that holds the slides and the rod (Figure 13a). The base was designed to slightly elevate the rod so that the mold makes a mostly circular shaped cavity, achieving the same shape as the macroscale actuator. The second component is the wall that is placed on top of the slides, where one edge is secured around the base, and the other edge has an extruded wall to create the rest of the cavity of the where the PU plastic is casted (Figure 13b). After 3D-printing the base and two walls, we inserted the rod (diameter, 3 mm) through the hole of the base and placed 1-mm thick slides on each slot in the base (Figure 13c). The cross-sectional view of the assembled mold is shown in Figure 13d.

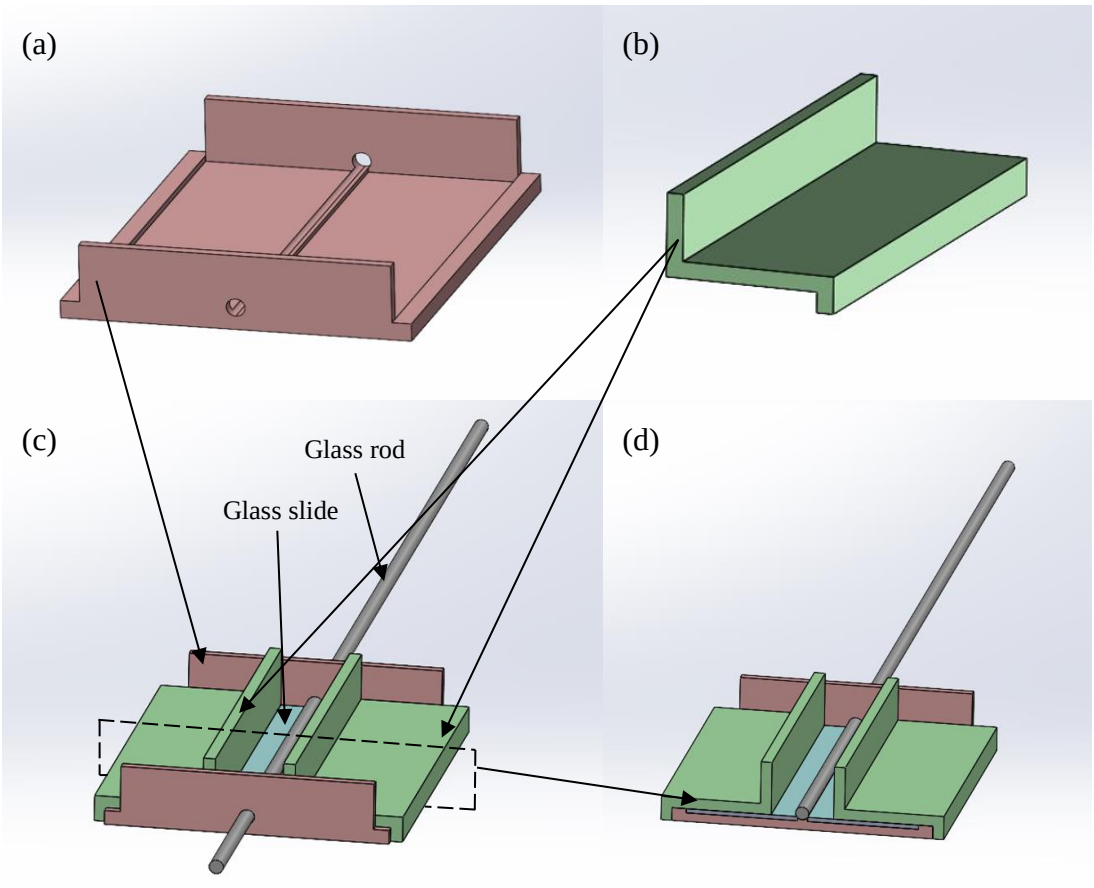

Figure 13. Mold components to create the PU plastic mold. (a) Main base to hold one glass slide on each side of the stand that holds the glass rod. (b) Wall that is placed on top on the slide and secured on the edge of the base. (c) Assembled mold, where the PU plastic will be casted in the cavity made by the green walls, rod, and slides. (d) Cross-sectional view of the assembled mold.

We prepared the PU plastic and poured it on top of the glass components in the mold until it reached the height of the walls and let it cure. Once the PU plastic mold was ready to be used as the silicone mold, we designed another mold to hold the PU plastic mold in place and allow a smaller glass rod (diameter, 1mm) to float in the center of the mold cavity (Figure 14). The mold to hold the PU plastic mold consists of the main bed (Figure 14b) to hold the PU plastic mold (Figure 14a) and a separate wall with a hole in the center that attaches to the main bed (Figure 14c). The purpose of the separate wall is to insert the 1 mm rod through the hole, place the rod on the silicone once the silicone is casted onto the PU plastic mold, and slide the

wall along the rod and attach the wall to the main bed (Figure 14d). The cross-sectional view of the mold to show the shape of the actuator is displayed in Figure 14e.

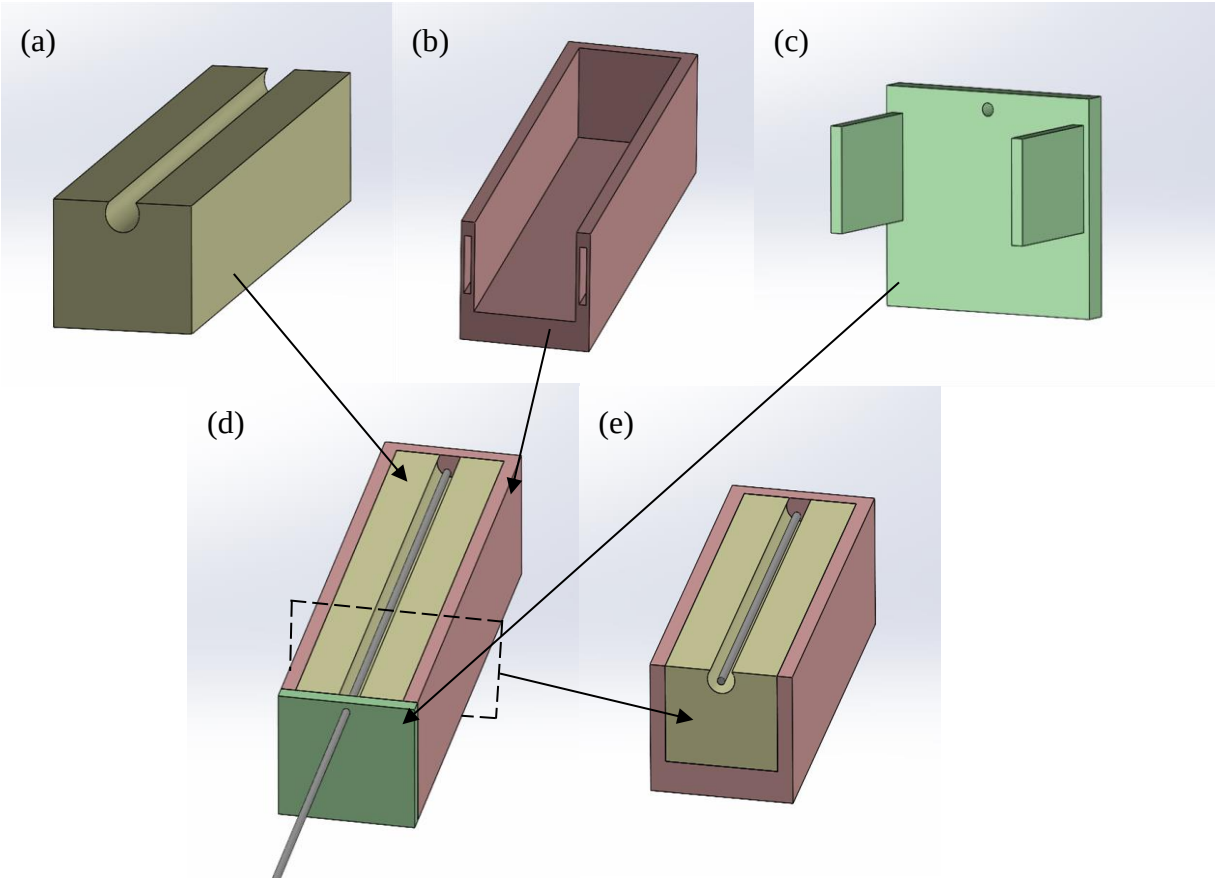

Figure 14. (a) PU plastic mold. (b) Main bed to hold PU plastic mold. (c) Cap that fits into the main bed with a hole near the top for the 1 mm rod to pass through and float in center of the PU plastic mold cavity. (d) Assembled mold. (e) Cross-sectional view of the mold.

After letting the silicone cure in the PU plastic mold, we retrieve the silicone actuator by detaching the wall from the main bed and sliding it off the rod. Then, we slowly remove the silicone from the PU plastic mold while the silicone is still wrapped around the rod. We follow the same procedure as we did for the macroscale actuator to attach the plastic bag sheet to the flat side of the actuator and to route the string around the actuator. We can obtain the final result by sliding the complete actuator off the rod.

Discussion of Outcome

The result of the progress we have for our microscale actuator fabrication procedure is shown in Figure 15.

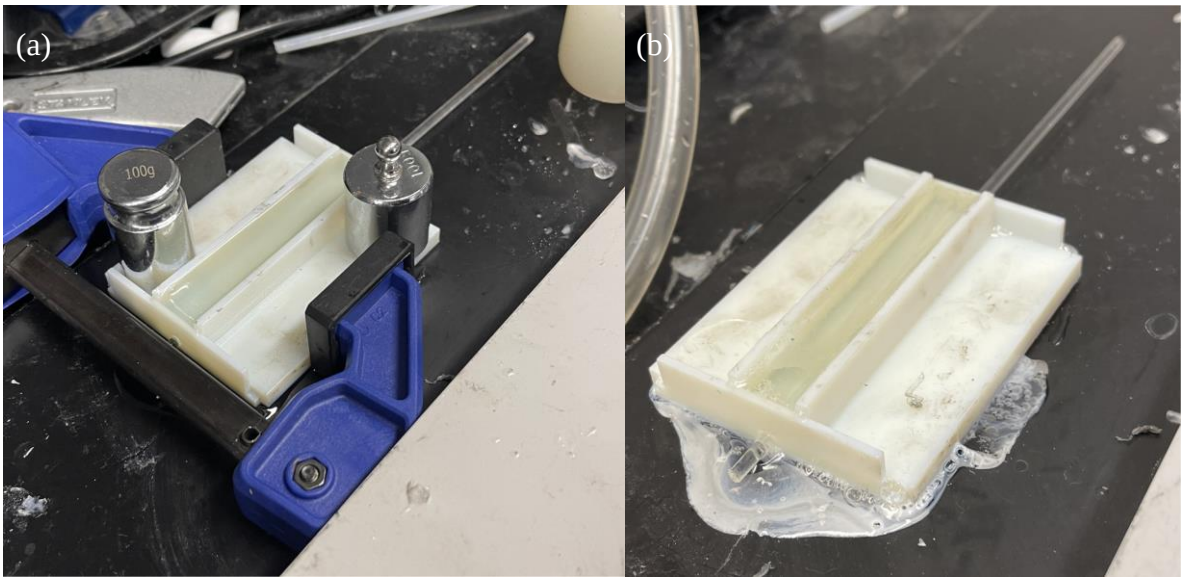

Figure 15. (a) Mold with the freshly casted PU plastic. The goal of clamping and adding weights to the mold was to prevent leaks on the sides. (b) Mold with cured PU plastic. The excess PU plastic on the surface is due to overflowing the mold with the PU plastic when initially casting.

The fabrication procedure is not finalized yet due to challenges we are facing with the PU plastic. Initially, when designing and printing the mold, the dimensions of the hole for the rod to slide through were not printed properly due to the tolerances of the 3D printer. As a result, the PU plastic would leak through the hole. After a few attempts of trial and error to determine the hole size, we were able to find a dimension that consistently printed a size to allow the rod to slide though without any room for leaks to occur.

Afterwards, we tried casting the PU plastic into the mold, but we have been unable to take the cured PU plastic out from the mold. Initially, the mold did not consist of multiple parts and the PU plastic mold was the length of the two slides and the 3 mm rod. The PU plastic would become stuck to the large surface area of the slides, which made it more difficult to remove the

PU plastic. Therefore, we introduced making walls so the PU plastic mold would take up less surface area and material. After a couple attempts of using the new mold, the PU plastic was still leaking under the wall and in between the slides. Additionally, we have been using Ease Release, a mold release to allow PU plastic to unbond from its mold (Smooth-On Inc., Macungie, PA, USA). However, the PU plastic in our most recent trial did not cure and remained slightly viscous. In our most recent trial, we added weights on top of the walls to prevent the PU plastic from flowing underneath the walls, and we eliminated the use of mold release to determine if the chemical properties of the mold release interfere with the curing process of PU plastic. The PU plastic cured properly since it became solid after the minimum curing time. However, the PU plastic remained stuck on the mold. We are looking into a new approach of casting and curing the PU plastic by lining the inside of the mold with a non-stick material, such as polytetrafluoroethylene (PTFE). However, more research on the properties of PTFE is required before proceeding with this new approach. Once we can consistently create the PU plastic mold and take it out from its mold it cured in, we can proceed to fabricating the microscale actuator with silicone.

CONCLUSION AND FUTURE DIRECTIONS

Our research introduced the design and fabrication of a hydraulic helical soft actuator to be applied to enhancing surgical catheters to remove PEs. Creating an actuator at the macroscale level allowed us to determine the optimal shape of the actuator, shape and size of the actuator chamber, types of materials that should be used, and determining the relationship between power supply and coiling. The way we fabricated our actuator using silicone, a piece of a plastic bag, and polyester string demonstrated that the actuator coils rapidly once at least 10 mL of air is supplied. Since our actuator demonstrated the greatest amount of coiling compared to previous prototypes, we moved forward to scaling down the actuator to a microscale size so that the actuator can fit within a pulmonary vein. We are following the same fabrication process except that the mold to cast silicone should be made with PU plastic due to the more compatible material properties of PU plastic when casting thin layers of silicone. However, we are in the process of determining the appropriate materials and mold design to create the PU plastic mold itself.

The next steps for our research is to continue working on the microscale actuator by determining whether PTFE lining on the mold for PU plastic will be the solution to taking the PU plastic out from the mold. Once we have our PU plastic mold, which will have the mostly circular-shaped cavity, we can place the PU plastic mold into the other mold to cast silicone into the PU plastic mold. The silicone mold has a place for a rod to float above the center of the cavity to create the power chamber of the actuator. Once the silicone is casted and cured in the mold, we can follow the same procedure of pasting the piece of a plastic bag onto the flat side of the actuator and routing the string. Another test can be done using the hydraulic power supply and EM tracker to determine whether the relationship between water supply and coiling

displacement is similar for the microscale actuator compared to the macroscale actuator. Then, once determining such a relationship, we would like to test the PE removal application by using a block of gelatin to simulate the blood clot in a 3D-printed plastic vessel, inserting the soft robot into the gelatin phantom, supplying a certain amount of water into the robot to break apart the gelatin, and removing the broken-up pieces of the gelatin using a suction machine. This simulation allows us to compare the removal efficiency between our robotic approach and a traditional approach involving guidewire puncture and suction to remove PEs.

REFERENCES

[1] Duffett, Lisa, et al. “Pulmonary Embolism: Update on Management and Controversies.” BMJ, 5 Aug. 2020, https://doi.org/10.1136/bmj.m2177.

[2] Lapner, S. T., and C. Kearon. “Diagnosis and management of pulmonary embolism.” *BMJ*, vol. 346, no. 757, 20 Feb. 2013, pp. 1–9, https://doi.org/10.1136/bmj.f757.

[3] Reyes, Guillermo, et al. “Surgical treatment of a massive pulmonary embolism after a double cardiac arrest.” *Revista Española de Cardiología (English Edition)*, vol. 60, no. 8, Jan. 2007, pp. 887–889, https://doi.org/10.1016/s1885-5857(08)60037-7.

[4] Douketis, James D., et al. “Clinical risk factors and timing of recurrent venous thromboembolism during the initial 3 months of anticoagulant therapy.” *Archives of Internal Medicine*, vol. 160, no. 22, 11 Dec. 2000, p. 3431, https://doi.org/10.1001/archinte.160.22.3431.

[5] Goldhaber, Samuel Z, et al. “Catheter-directed thrombolysis for deep vein thrombosis: 2021 update.” *Vascular Medicine*, vol. 26, no. 6, 4 Oct. 2021, pp. 662–669, https://doi.org/10.1177/1358863x211042930.

[6] Douketis, James D., Jeffery S. Ginsberg, et al. “Risk of fatal pulmonary embolism in patients with treated venous thromboembolism.” *JAMA*, vol. 279, no. 6, 11 Feb. 1998, pp. 458–462, https://doi.org/10.1001/jama.279.6.458.

[7] Sedhom, Ramy, et al. “Contemporary National Trends and outcomes of pulmonary embolism in the United States.” *The American Journal of Cardiology*, vol. 176, Aug. 2022, pp. 132–138, https://doi.org/10.1016/j.amjcard.2022.03.060.

[8] Fleck, Drew, et al. “Catheter-directed thrombolysis of deep vein thrombosis: Literature Review and practice considerations.” *Cardiovascular Diagnosis and Therapy*, vol. 7, no. S3, Dec. 2017, https://doi.org/10.21037/cdt.2017.09.15.

[9] Martin, Colleen, et al. “Systemic Thrombolysis for Pulmonary Embolism: A Review.” *P & T : A Peer-Reviewed Journal for Formulary Management*, U.S. National Library of Medicine, Dec. 2016, www.ncbi.nlm.nih.gov/pmc/articles/PMC5132419/.

[10] Silver, Mitchell J., et al. “Outcomes in high-risk pulmonary embolism patients undergoing flowtriever mechanical thrombectomy or other contemporary therapies: Results from the flame study.” *Circulation: Cardiovascular Interventions*, vol. 16, no. 10, 17 Oct. 2023, https://doi.org/10.1161/circinterventions.123.013406.

[11] Huang, Yi-xiong, et al. “Angiojet rheolytic thrombectomy in patients with thrombolysis in myocardial infarction Thrombus Grade 5: An observational study.” *Scientific Reports*, vol. 12, no. 1, 31 Mar. 2022, https://doi.org/10.1038/s41598-022-09507-z.

[12] Schubert, Franziska, et al. “Comparison of aspiration catheters with modified standard catheters for treatment of large pulmonary embolism using an in-vitro patho-physiological model.” *CardioVascular and Interventional Radiology*, vol. 45, no. 1, 18 Nov. 2021, pp. 112–120, https://doi.org/10.1007/s00270-021-02987-y.

[13] Schultz, Jacob, et al. “Catheter-based therapies in acute pulmonary embolism.” *EuroIntervention*, vol. 13, no. 14, Feb. 2018, pp. 1721–1727, https://doi.org/10.4244/eij-d-17-00437.

[14] Sobieszczyk, Piotr. “Catheter-assisted pulmonary embolectomy.” *Circulation*, vol. 126, no. 15, 9 Oct. 2012, pp. 1917–1922, https://doi.org/10.1161/circulationaha.110.963041.

[15] Hijikata, Ryojiro, et al. “Evaluation of mechanical properties of catheter shafts under cyclic bending.” *MATERIALS TRANSACTIONS*, vol. 58, no. 7, 2017, pp. 1049–1054, https://doi.org/10.2320/matertrans.p-m2017816.

[16] Kilic, A., et al. “Nationwide outcomes of surgical embolectomy for acute pulmonary embolism.” *Journal of Vascular Surgery*, vol. 58, no. 1, July 2013, p. 277, https://doi.org/10.1016/j.jvs.2013.05.039.

[17] Thai, Mai Thanh, et al. “Advanced Intelligent Systems for Surgical Robotics.” Advanced Intelligent Systems, vol. 2, no. 8, 2020, p. 1900138., https://doi.org/10.1002/aisy.201900138.

[18] Hu, Weiping, et al. “3D Printed Helical Soft Pneumatic Actuators.” 2018 IEEE/ASME International Conference on Advanced Intelligent Mechatronics (AIM), 2018, https://doi.org/10.1109/aim.2018.8452456.

[19] Alici, Gursel. “Softer Is Harder: What Differentiates Soft Robotics from Hard Robotics?” MRS Advances, vol. 3, no. 28, 2018, pp. 1557–1568., https://doi.org/10.1557/adv.2018.159.

[20] Coyle, Stephen, et al. “Bio-inspired Soft robotics: Material selection, actuation, and Design.” *Extreme Mechanics Letters*, vol. 22, July 2018, pp. 51–59, https://doi.org/10.1016/j.eml.2018.05.003.

[21] Majidi, Carmel. “Soft-matter engineering for Soft Robotics.” *Advanced Materials Technologies*, vol. 4, no. 2, 13 Dec. 2018, https://doi.org/10.1002/admt.201800477.

[22] Rosalia, Luca, et al. “Geometry-based customization of bending modalities for 3D-printed soft pneumatic actuators.” *IEEE Robotics and Automation Letters*, vol. 3, no. 4, Oct. 2018, pp. 3489–3496, https://doi.org/10.1109/lra.2018.2853640.

[23] Galloway, Kevin C., et al. “Soft Robotic grippers for biological sampling on Deep Reefs.” *Soft Robotics*, vol. 3, no. 1, Mar. 2016, pp. 23–33, https://doi.org/10.1089/soro.2015.0019.

[24] Yang, Xinyu, et al. “Multidirectional bending soft pneumatic actuator with fishbone-like strain-limiting layer for dexterous manipulation.” *IEEE Robotics and Automation Letters*, vol. 9, no. 4, Apr. 2024, pp. 3815–3822, https://doi.org/10.1109/lra.2024.3369475.

[25] Gopesh, Tilvawala, et al. “Soft robotic steerable microcatheter for the endovascular treatment of cerebral disorders.” *Science Robotics*, vol. 6, no. 57, 11 Aug. 2021, https://doi.org/10.1126/scirobotics.abf0601.